Journal of Coastal Research	SI 56	467 - 471	ICS2009 (Proceedings)	Portugal	ISSN 0749-0258

Euler–Euler Coupled Two-Phase Flow Modeling of Sheet Flow Sediment Motion in the Nearshore

R. Bakhtyar†, A. Yeganeh-Bakhtiary‡, D.A. Barry† and A. Ghaheri‡

† Faculté de l'environnement naturel, architectural et construit, Ecole polytechnique fédérale de Lausanne, Switzerland
roham.bakhtyar@epfl.ch
andrew.barry@epfl.ch

‡ Department of Civil Engineering, Iran University of Science and Technology, Tehran, Iran
yeganeh@iust.ac.ir
ghaheri@iust.ac.ir

ABSTRACT

BAKHTYAR, R., YEGANEH-BAKHTIARY, A., BARRY, D.A. and GHAHERI A., 2009. Coastal processes on a low energy beach. Journal of Coastal Research, SI 56 (Proceedings of the 10th International Coastal Symposium), 467–471. Lisbon, Portugal, ISSN 0749-0258.

A two-dimensional numerical model was presented for the simulation of sediment transport under oscillatory sheet flow conditions in the nearshore zone. Most existing mathematical models for predicting sediment transport in this area are based on the governing equations for single-phase flow. Considering the fact that the intergranular stress and the interaction between fluid and sediment are the predominant forcing mechanisms in the nearshore zone, a more realistic approach is to treat the fluid and sediment as a two-phase flow. In this paper, we present an Eulerian two-phase flow model for fluid–sediment sheet-flow simulation. All the most important forcing terms such as the fluid/particle and particle/particle interactions as well as the turbulent stresses are included in the model. The generation, translation and dissipation of turbulence can be modeled appropriately. The model predictions compared well with the experimental data.

ADITIONAL INDEX WORDS: *Sediment concentration, Numerical simulation, Oscillatory flow*

INTRODUCTION

An important task for coastal engineers is to predict sediment transport rates in coastal regions. Severe beach topography changes often take place during stormy wave conditions when the sheet flow mode of transport is predominant. The sheet flow mode refers to bed-load transport at high bottom shear stress, for which sediment transport occurs in a layer very close to the bed with a thickness of several times of the particle diameter.

The location of particles in sheet flow conditions is defined by the collision and the contact of the grains, which differs from the usual turbulence generated suspension (Bagnold, 1954). Due to the many phenomena affecting sediment transport in the nearshore zone and the difficulties encountered in field measurements, there still is much to be investigated about the hydrodynamics and sediment transport of this zone. Among the main processes, the least well-understood and most difficult to predict is the dynamics of near-bed sediment motions on beaches. Since the sheet flow is a highly concentrated combined flow of fluid and sediments under periodic motion; the understanding of mechanisms that govern the sediment transport is extremely complicated.

Over the past two decades much research has been carried out to achieve a better understanding of sheet flow. Despite significant recent advances in experimental techniques, laboratory experiments and field studies still have their own difficulties and limitations. In addition to the high cost of experiments, laboratory experiments suffer from constraints in the range of applicable physical parameters and scaling effects. Field studies are limited to site access and environmental variability. The difficulties and limitations of field and laboratory experiments along with the rapid advancement in computational power have led to the growing popularity of numerical simulation of sediment transport in sheet flow in recent years.

Numerical simulations are able to provide detailed insights into flow and turbulence structures without facing any difficulties of scaling and measuring. As shown by recent experimental and numerical studies, the conventional models, whether based on the turbulent diffusion concept making use of an empirically derived bottom reference concentration as the boundary condition or the "energetic" concept (Bagnold, 1954), are too simplistic to truly represent the unsteady, nonlinear and two-phase nature of the sediment motions. Most mathematical models presented for sediment transport in oscillatory flows are based on the assumption of single-phase flow (Nadaoka and Yagi, 1990; Davies *et al.*, 2002). These models are not suitable for the prediction of velocity and concentrations that vary with time. For sheet flow conditions, a more practical description about the physical mechanisms is needed to improve understanding nearshore sediment transport.

Numerical models, which are based on two-phase flow modeling, allow detailed flow and sediment fields to be resolved, while turbulence generation, advection and dissipation can be well simulated by incorporating a turbulence closure model into such models.

In the Euler-Euler coupling model, by averaging the sediment motions, the sediment phase can be treated as a continuum, which follows different constitutive laws to those of the clear water. Asano (1990) presented a two-phase flow model based on the principles of the Kobayashi and Seo (1985) model in which the vertical velocity of particles was approximated by empirical relations. Dong and Zhang (1999) presented a two-phase flow model capable of simulating fluid and particle motions in sheet flow and oscillatory conditions. They used the eddy viscosity model although it is restricted for modeling this complex flow. Hsu *et al.* (2003, 2004a) applied a two-phase flow model to unsteady oscillatory flow. Using a two-phase model, Hsu and Hanes (2004b) examined the effects of wave shape on sediment transport. They found that for certain wave shapes, time-dependent sediment transport cannot be completely parameterized by the instantaneous free-stream velocity. Liu and Sato (2006) applied a two-phase flow model based on Liu and Sato (2005) to simulate the net transport rate under combined wave-current flow and various asymmetric sheet flow conditions. Their turbulent enclosure model was based on the parabolic eddy viscosity distribution. Li *et al.* (2008) presented a two-phase flow numerical model, which is based on one-equation k-closure for turbulence. They used the free-stream velocity profile according to the wave theory to simulate sediment transport under wave sheet flow conditions.

Considering that inter-granular stresses and the interaction between fluid and sediment are predominant forcing mechanisms in sheet flow, an accurate approach is to treat the fluid and sediment as two-phase flow. Validation of such a modeling approach should include comparisons with hydrodynamic data for the fluid, sediment and turbulent field.

In this study, a combination of a comprehensive two-phase flow model, based on the Euler-Euler coupling of the governing equations for the sediment and fluid phases, with a k–ε turbulence model has been used to study the sediment transport in sheet flow conditions. Finite difference solutions to the two-phase flow model and the k–ε model are obtained, while waves are generated by using of internal source functions inside the computational domain. Each of the two phases is defined via the Navier-Stokes equations. The coupling between the phases is performed considering the interaction between the fluid and sediment phases via the momentum conservation equations. Unlike most previous investigations that solved the one-dimensional boundary layer equation of motion, the present model solves the full two-phase flow model in the entire domain. Here, the 2D governing equations are implemented in the vertical plane.

COMPUTATIONAL MODEL

Two-phase flow modeling is capable of simulating coupled fluid and sediment phases separately. There are two methods for coupling: (i) one-way coupling model where the fluid flow affects the sediment phase but not vice versa, and (ii) two-way coupling each phase affects the other. The one-way coupled approach is used here.

The 2D governing equations of the fluid and sediment phases are implemented in the vertical plane as follows (Bakhtyar *et al.*, 2009):

$$\frac{\partial(1-C)}{\partial t}+\frac{\partial(1-C)U_x}{\partial x}+\frac{\partial(1-C)U_z}{\partial z}=0; \tag{1}$$

$$\frac{\partial C}{\partial t}+\frac{\partial CV_x}{\partial x}+\frac{\partial CV_z}{\partial z}=0; \tag{2}$$

$$\begin{aligned}&\frac{\partial(1-C)U_x}{\partial t}+U_x\frac{\partial(1-C)U_x}{\partial x}+U_y\frac{\partial(1-C)U_x}{\partial z}-U_x\frac{\partial\overline{C'U'_x}}{\partial x}\\&-U_x\frac{\partial\overline{C'U'_z}}{\partial z}=g(1-C)-\frac{(1-C)}{\rho_f}\frac{\partial P}{\partial x}+\frac{\partial}{\partial x}\left(2\Gamma\frac{\partial U_x}{\partial x}\right)(1-C)\\&+\frac{\partial}{\partial z}(1-C)\Gamma\left(\frac{\partial U_z}{\partial x}+\frac{\partial U_x}{\partial z}\right);\end{aligned} \tag{3}$$

$$\begin{aligned}&\frac{\partial(1-C)U_z}{\partial t}+U_z\frac{\partial(1-C)U_z}{\partial z}+U_x\frac{\partial(1-C)U_z}{\partial x}\\&-U_z\frac{\partial\overline{C'U'_z}}{\partial z}-U_z\frac{\partial\overline{C'U'_x}}{\partial x}=-\frac{(1-C)}{\rho_f}\frac{\partial P}{\partial z}+\\&\frac{\partial}{\partial z}\left(2\Gamma\frac{\partial U_z}{\partial z}\right)(1-C)+\frac{\partial}{\partial x}(1-C)\Gamma\left(\frac{\partial U_z}{\partial x}+\frac{\partial U_x}{\partial z}\right);\end{aligned} \tag{4}$$

$$\begin{aligned}&\frac{\partial CV_x}{\partial t}+V_x\frac{\partial CV_x}{\partial x}+V_y\frac{\partial CV_x}{\partial x}+V_x\frac{\partial\overline{C'V'_x}}{\partial x}+V_x\frac{\partial\overline{C'V'_y}}{\partial y}=gC\\&-\frac{C}{\rho_s}\frac{\partial P}{\partial x}+\frac{\partial}{\partial x}\left(2\nu_t\frac{\partial V_z}{\partial x}\right)C+\frac{\partial}{\partial y}C\nu_t\left(\frac{\partial V_z}{\partial x}+\frac{\partial V_x}{\partial y}\right)\\&+\frac{\partial T_{xy}}{\partial z}-\frac{f_{dx}}{\rho_f};\end{aligned} \tag{5}$$

$$\begin{aligned}&\frac{\partial CV_z}{\partial t}+V_z\frac{\partial CV_z}{\partial z}+V_x\frac{\partial CV_z}{\partial x}+V_z\frac{\partial\overline{C'V'_z}}{\partial z}+V_z\frac{\partial\overline{C'V'_x}}{\partial x}=\\&-\frac{C}{\rho_s}\frac{\partial P}{\partial z}+\frac{\partial}{\partial z}\left(2\nu_t\frac{\partial V_z}{\partial z}\right)C+\frac{\partial}{\partial x}C\nu_t\left(\frac{\partial V_z}{\partial x}+\frac{\partial V_x}{\partial z}\right)\\&+\frac{\partial T_{xx}}{\partial z}-\frac{f_{dz}}{\rho_f};\end{aligned} \tag{6}$$

where (U_x,U_y) and (V_x,V_z) are the fluid and sediment particle velocities, respectively; T_{ij} is the inter-granular stress tensor; C is the sediment phase volume concentration; P is the pressure; g is the magnitude of gravitational acceleration; ρ_f and ρ_s are the fluid and sediment densities, respectively; U', V' and C' are the fluctuating components of the fluid velocities and sediment concentration; $\Gamma=\nu_t+\nu$; ν is the kinematic viscosity and ν_t is the eddy viscosity. The hydrodynamic force (f_d) exerted on the particulate phase is (Hsu *et al.*, 2003):

$$f_d=C\rho_f\left[\frac{3}{4}C_D\frac{1}{d_{50}}(\mathbf{U}-\mathbf{V})\sqrt{(\mathbf{U}-\mathbf{V})^2+(\mathbf{U}-\mathbf{V})^2}\right]; \tag{7}$$

where **U** and **V** are the velocity vector of the fluid and sediment phases, d_{50} is the median particle diameter, C_D is the drag coefficient. The drag coefficient is (Dong and Zhang, 1999):

$$C_D = \left[\frac{24\nu}{d_{50}\sqrt{(U_x - V_x)^2 + (U_z - V_z)^2}} + 2 \right] (1 - C)^{-4.5}; \tag{8}$$

The relation between the Reynolds stresses and the rate of flow shape change as follows (Longo, 2005):

$$\overline{U_i' U_j'} = -\nu_t (U_{i,j} + U_{j,i}) + \frac{2}{3}\delta_{ij} k - \frac{2}{3}\nu_t \delta_{ij} U_{j,i}; \tag{9}$$

$$\overline{C' U_i'} = \overline{C' V_i'} = -\frac{\nu_t}{Sc_c} C; \tag{10}$$

We use the two-equation turbulence model for predicting two-phase flows that was developed by Elghobashi and Abou-Arab (1983). The transformation equations for k and ε are, respectively (Longo, 2005):

$$\frac{Dk}{Dt} = \frac{\partial}{\partial x_i}\left[\left(\nu + \frac{\nu_t}{\sigma_k} \right) \frac{\partial k}{\partial x_i} \right] + \nu_t \left(\frac{\partial U_i}{\partial x_j} + \frac{\partial U_j}{\partial x_i} \right) \frac{\partial U_i}{\partial x_j} + \frac{\rho_s - \rho}{\rho} g \nu_t \frac{\partial C}{\partial y} - \varepsilon - \nu_t \frac{\partial C}{\partial y} F_d; \tag{11}$$

$$\frac{D\varepsilon}{Dt} = \frac{\partial}{\partial x_i}\left[\left(\nu + \frac{\nu_t}{\sigma_\varepsilon} \right) \frac{\partial \varepsilon}{\partial x_i} \right] + C_{1\varepsilon} \frac{\varepsilon}{k} \nu_t \left(\frac{\partial U_i}{\partial x_j} + \frac{\partial U_j}{\partial x_i} \right) \frac{\partial U_i}{\partial x_j} + C_{2\varepsilon} g \nu_t \frac{\varepsilon}{k} \frac{\rho_s - \rho}{\rho} \frac{\partial C}{\partial y} - C_{3\varepsilon}\varepsilon - \nu_t F_d \frac{\varepsilon}{k} \frac{\partial C}{\partial y}_d; \tag{12}$$

$$F_d = \frac{C}{1 - C} \frac{3C_{De}}{4d} |\mathrm{U} - \mathrm{V}|^2; \tag{13}$$

$$C_{1\varepsilon} = 1.44,\; C_{2\varepsilon} = 1.92,\; C_{3\varepsilon} = 1.2,\; C_{4\varepsilon} = 1.92; \tag{14}$$

Collisional stresses for the sediment phase

The stresses generated by particle collisions have significant effects on the velocities of both phases. Savage and McKewon (1983) presented the following equation based on their experiments:

$$T_{xz} = 1.2\lambda^2 \nu \rho_f \frac{\partial V_x}{\partial z},\; \lambda = \left[(C_m / C)^{\frac{1}{3}} - 1 \right]^{-1}; \tag{15}$$

where C_m is the maximum sediment concentration. The normal inter-granular stress is related to the tangential stress by:

$$T_{zz} = T_{xz} \cot\phi; \tag{16}$$

in which ϕ is the static angle of repose.

Fluid and sediment initial and boundary conditions

The initial conditions are a zero velocity for fluid and sediment and a hydrostatic pressure distribution. In this model both fluid and sediment particle velocity components are considered zero at the bottom boundary (no-slip boundary condition). Both sides of the calculating domain are periodic. The sediment concentration at bottom boundary is taken as the maximum concentration (C_m = 0.60). To conserve the sediment mass, a zero flux condition is used for the sediment concentration calculation at the top sheet flow boundary as follows (Liu and Sato, 2006):

$$V_z C - \nu_t \frac{\partial C}{\partial z} = 0; \tag{17}$$

NUMERICAL RESULTS AND DISCUSSION

The numerical two-phase model described has been compared with the experimental results reported by Asano (1995). The experiments were performed in a piston-driven oscillatory flow tank. The flow section is 2.5-m high and 8-m long. Sediments were placed along the bottom of the tank. Table 1 reports the problem's input parameters, where T is the wave period. Although the inception of sheet flow conditions is not well established, usually, sheet flow occurs when the Shields parameter exceeds about 0.6 (Horikawa *et al.*, 1982). But in Asano (1995), the sheet flow condition started below this criterion. Asano (1995) provided the possible explanation of lower inception of sheet flow condition, stating that it is likely due to the fact that "the particles used herein were nearly spherical, unlike natural sand" and has a smaller density than natural sand.

In Fig. 1, the model results are compared with vertical profiles of sediment concentration for the experiment at different times. The panels show sediment concentration at $\theta = 5\pi/3$, $\pi/6$, $\pi/3$, $\pi/2$ and $2\pi/3$. Even though a slight difference can be seen between measured and predicted results, overall the agreement is excellent. As shown in Fig. 1, the sediment concentration profile shows an upward convex shape in the velocity distribution near the original bed, indicating on the presence of a sheet-flow motion of moving particles.

Sediment fluxes were computed by multiplication of the sediment particle velocities and the sediment concentrations. Figure 2 shows the comparison between measured and calculated vertical distribution of sediment flux at different oscillatory phases ($\theta = \pi/6$, $\pi/3$, $\pi/2$ and $2\pi/3$). The numerical solutions are presented for a single point in the x direction because the averaged flow in oscillatory wave tunnel is purely horizontal. In agreement with the measurements the numerical model predicts a similar profile of sediment flux as the waves propagate. It can be seen from Fig. 2 that the sediment flux in the sheet flow layer is much larger than in the overlying layer. Meanwhile, the sediment fluxes increase towards the initial bed level and decrease over a thin layer above the initial bed level. The differences between the numerical results and experimental data may due to different physical processes in oscillatory wave tunnel and numerical wave propagation. Oscillatory wave tunnels are not a realistic representation of coastal water waves. Lin and Zhang (2008) pointed out the main reason for this disagreement is that in the experimental research using oscillatory wave tunnels, the flow is uniform in the horizontal direction, which is not the real case for water waves except the wave length is very long. Furthermore, in the wave tunnel, the free surface was neglected unlike the problem under real waves.

Table 1: Basic characteristics of experiment (Asano, 1995)

Shields parameter	*T* (s)	Maximum velocity (cm s^{-1})
0.532	4.64	85

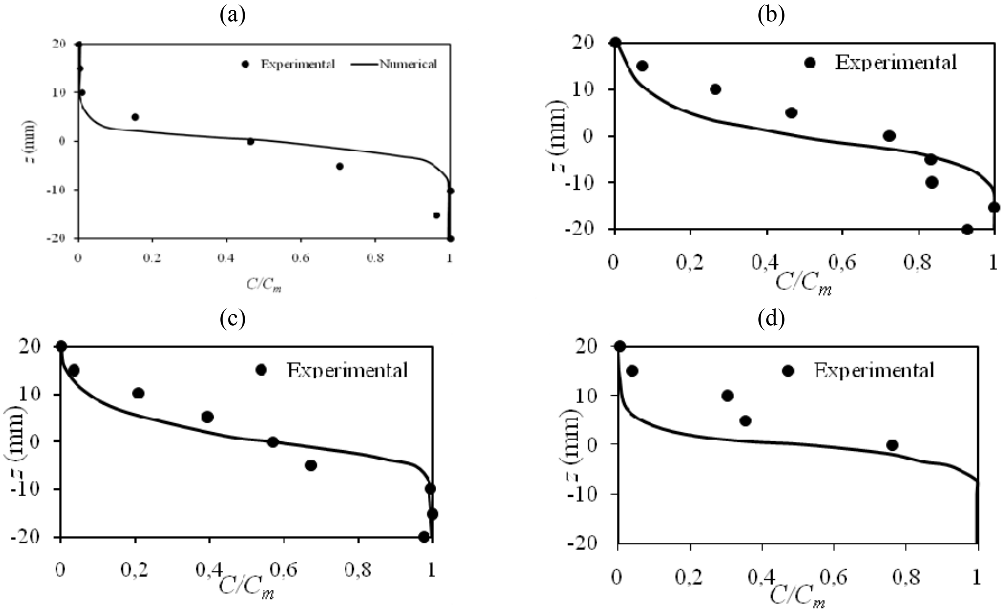

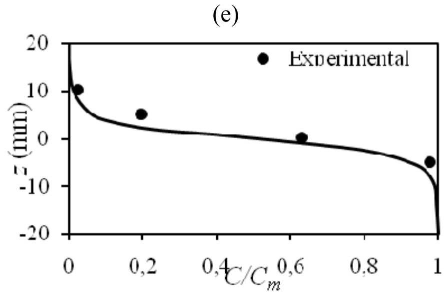

Figure 1. Vertical distribution of sediment concentration. Solid symbols are the experimental data (Asano, 1995) and solid lines are the numerical results. The panels show sediment concentration at θ= (a)$\pi/6$; (b)$\pi/3$; (c)$\pi/2$; (d)$2\pi/3$ and (e) $5\pi/3$.

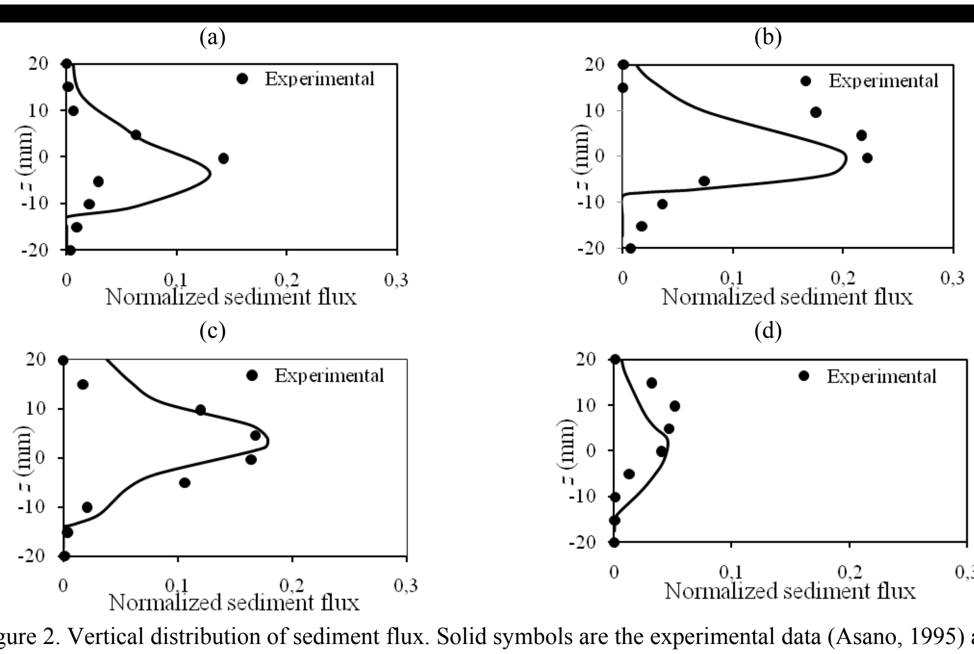

Figure 2. Vertical distribution of sediment flux. Solid symbols are the experimental data (Asano, 1995) and solid lines are the numerical results. The panels show sediment concentration at θ= (a)$\pi/6$; (b)$\pi/3$; (c)$\pi/2$ and (d) $2\pi/3$.

CONCLUSIONS

In this study, a time-dependent comprehensive computational fluid dynamic model was developed to improve understanding of the two-dimensional sediment transport in the sheet flow under non-breaking waves. The model is based on the two-phase flow equations for reciprocating flows in the sheet flow based on the mass and momentum conservation equations for both the sediment and the fluid phases, and the two-equation k-ε turbulence model. This study has led to a better understanding of several important issues related to the assessment of two-phase flow model for simulating sediment under oscillatory sheet flow conditions. The model can be extended to investigate real wave-induced sheet flow conditions.

Model performance of the model was evaluated by comparing numerical solutions with the experimental data of Asano (1995) for oscillatory flow. Generally, there is good agreement between the results of the model and experimental data. According to the analysis of this study, the following conclusions are drawn:

- Results show that sediment flux is a maximum in the sheet flow layer near the initial bed level.
- The sediment flux increases towards the initial bed level and decreases over a thin layer above the initial bed level.
- The sediment concentration profile shows an upward convex shape of the velocity distribution near original bed. With increased height the velocity profile changes smoothly its shape into an upward concave curve.
- Generally, the important features of wave-generated sheet flow characteristics are well described by the flow model.

LITERATURE CITED

ASANO, T., 1990. Two-phase flow model on oscillatory sheet-flow. *Proceedings of 22nd International Conference on Coastal Engineering*, ASCE, New York; pp. 2372-84.

ASANO, T., 1995. Sediment transport under sheet-flow conditions. *Journal of Water, Port, Coast, and Ocean Engineering,* 21(5), 239-246.

BAGNOLD, R.A., 1954. Experiments on a gravity-free dispersion of large solid spheres in a Newtonian fluid under shear. *Proc Roy Soc London*, 49–63.

BAKHTYAR, R., YEGANEH-BAKHTIARY, A., BARRY, D.A. and GHAHERI, A., 2009. Two-phase hydrodynamic and sediment transport modeling of wave-generated sheet flow. *Advances in Water Resources*, Submitted.

DAVIES, A.G., VAN RIJN, L.C., DAMGAARD, J.S., VAN DE GRAAFF, J. and RIBBERINK, J.S., 2002. Intercomparison of research and practical sand transport models. *Coastal Engineering*, 46, 1-23.

DONG, P. and ZHANG, K., 1999. Two-phase flow modeling of sediment motions in oscillatory sheet flow. *Coastal Engineering*, 36, 87-109.

ELGHOBASHI, S.E. and ABOU-ARAB, T.W., 1983. A two-equation turbulence model for two-phase flows. *Physics of Fluids,* 26, 931–38.

HSU, T. CHANG, H. and HSIEH, C., 2003. A two-phase flow model of wave-induced sheet flow. *Journal of Hydraulic Research,* 41, 299-310.

HSU, T, JENKINS, J.T. and LIU, P., 2004. On two-phase sediment transport: Sheet flow of massive particles. *Proc Roy Soc London A,* 460, 2223-50.

HSU, T. and HANES, D.M., 2004. Effects of wave shape on sheet flow sediment transport. *Journal of Geophysical Research,* 109, C05025, doi: 10.1029/2003JC002075.

KOBAYASHI, N. and SEO, S.N., 1985. Fluid and sediment interaction over a plane bed. *Journal of Hydraulic Engineering,* 111, 903-21.

LIN, P. and ZHANG, W., 2008. Numerical simulation of wave-induced laminar boundary layers. *Coastal Engineering,* 55, 400-408.

LI, M. PAN, S. and O'CONNOR, BA., 2008. A two-phase numerical model for sediment transport prediction under oscillatory sheet flow. *Coastal Engineering,* 55, 1159-73.

LIU, H. and SATO, S., 2005. Modeling sediment movement under sheet flow conditions using a two-phase flow approach. *Coastal Engineering Japan,* 47, 255–84.

LIU, H. and SATO, S., 2006. A two-phase flow model for asymmetric sheet flow conditions. *Coastal Engineering,* 53, 825-43.

LONGO, S., 2005. Two-Phase Flow Modeling of Sediment Motion in Sheet-Flows above Plane Beds. *Journal of Hydraulic Engineering,* 131, 366-379.

NADAOKA, K. and YAGI, H., 1990. Single-phase fluid modeling of sheet-flow toward the development of numerical mobile bed. *Proceedings of 22nd International Conference on Coastal Engineering*, ASCE; pp. 2346-59.